Synthesis of EVA-g-MAH and its compatibilization effect to PA11/PVC blends

Tao Wang · Dan Liu · Chuanxi Xiong

Abstract Ethylene vinyl acetate (EVA) was grafted with maleic anhydride (MAH) to get terpolymer of EVA-g-MAH, and then was employed as a reactive compatibilizer to develop PA11/PVC blends. Mechanical properties indicate the critical EVA-g-MAH content at about 15 wt% and the blending of PVC with PA11 reserves PA11s high performance even at high PVC incorporation. The glass transition temperature change by DMA proves the compatibilization effect. SEM micrographs reveal that PA11/PVC blends have a two-phase structure. Particularly, PA11 is the continuous phase and PVC is the dispersed phase. PVC disperses uniformly in PA11 phase in the presence of EVA-g-MAH, and the increasing PA11 content leads to further decrease of PVC domain size. PA11/PVC blends are compatibilized by in situ reaction between PA11 and EVA-g-MAH, as well as intermolecular specific interactions between EVA-g-MAH and PVC.

Introduction

Ethylene vinyl acetate copolymer (EVA) is a random copolymer consists of ethylene and vinyl acetate (VA) as the repeating unit [1]. Ethylene unit is nonpolar and crystallizable, whereas vinyl acetate is polar and noncrystallizable. Random incorporation of the vinyl acetate unit into polyethylene progressively hinders the ability of the polymer to crystallize. The properties of EVA copolymers depend on their vinyl acetate (VA) contents [2]. Products with different VA content are used in different applications. EVA varies from plastics to elastics and adhesives. For example, copolymers with low VA content (<20%) are usually employed as thermoplastics, whereas those with high levels of VA are generally considered as oil-resistant elastomers [3, 4]. Another example of the influence of VA content on the application of EVA is EVA/PVC blend. Addition of EVA was found to improve low temperature impact strength as well as process ability of PVC since 1970s. Miscibility of EVA with PVC depends on the ethylene/vinyl acetate ratio. PVC blends with EVA comprising less than 30 wt% VA are highly immiscible, showing low toughening effect and poor impact strength. Blends of PVC with EVA comprising at least 50 wt% VA behave as miscible. The optimum VA content seems to be about 40–45 wt%.

A relatively easy and cost-effective way to produce new combinations of properties is blending. However, most blends achieved by melt mixing are immiscible and thus show poor properties. Therefore, compatibilization is demanded to obtain a blend with desired properties [5]. Grafting reaction by reactive monomers, such as vinyl silane [6], acrylic acid (AA) [7], or maleic anhydride (MAH) [8, 9], on the main chain of a polymer in the presence of peroxide could be achieved. When a graft copolymer possessing functional groups reacts with a polymer, such as poly(butylene terephthalate) (PBT), poly(ethylene

T. Wang (✉) · D. Liu
Department of Physics, University of Surrey,
Guildford, Surrey GU2 7XH, UK
e-mail: t.wang@surrey.ac.uk

C. Xiong
School of Materials Science and Engineering, Wuhan
University of Technology, Wuhan 430070, P.R. China

terephthalate)(PET), or nylon containing –OH, –COOH or NH$_2$ groups on the chain end, a desired compatibilizer to improve the compatibility between two different polymers is produced through in situ reaction under the condition of a high temperature and shearing. The compatibilizer produced by the reactive compatibilization exhibits more improved interfacial adhesion in blends than a common physical compatibilizer [5]. Recently, the reactive compatibilizers have been extensively investigated to overcome the poor properties of blends. It has been proved by many researchers that the amine end groups of Polyamides can react with anhydride functionality of maleic anhydride and in situ form grafting copolymer at the interface [10–13]. Maleic anhydrides are effective compatibilizers for many polymer blends.

Another way to overcome the compatibilization is the development of specific interactions such as hydrogen bonding, dipole–dipole, ion–dipole, charge transfer and transition metal complexation by introducing specific functional groups to the polymers [14–21]. Jiang et al. [22] studied the interpolymer complexation and miscibility enhancement by hydrogen bonding. Liu et al. [23] investigated graft-like hydrogen bonding complexes based on pyridyl-containing polymers and end-functionalized polystyrene oligomers. Several studies have been carried out concerning the miscibility behavior of polymers bearing polar groups and polyamides [24–26]. Researches show that PVC (hydrogen bonds donor) is miscible with hydrogen bonds acceptor polymers [27–31]. Olabisi et al. [31] pointed out that the reason of ethylene/ethyl acrylate or ethylene-vinyl-acetate copolymer is miscible with PVC was attributed to the special interaction between carbonyl group(hydrogen bonds acceptor) in these copolymers and α-hydrogen(hydrogen bonds donor) of PVC. Robeson et al. [32] investigated the compatibility between PBT and PVC, and attributed the compatibility to the interaction of ester carbonyl and α-hydrogen of PBT and PVC, respectively.

Polyamide11, one of the odd polyamides, is an important engineering thermoplastic. Poly (vinyl chloride) (PVC) is a widely used thermoplastic due to its exceptional corrosion resistance, self-extinguishability, flame resistance, inexpensiveness and recoverability. The blends of vinyl halide or vinylidene halide polymer and polyamide together can give tough, flexible, chemically resistance compositions suitable for wire and cable jacketing and chemically resistant liners [33].

This investigation is focused on the synthesis of EVA-g-MAH and its application as a compatibilizer to provide reaction compatibilization and intermolecular specific interactions compatibilization to the blends.

Experimental

Materials

Two kinds of EVA were used to graft with maleic anhydride, provided by Hyundai Co. (Korea) with 18% VA content and Exxon Co. (USA) with 40% VA content, respectively. Maleic anhydride was supplied by BASF Co. (Germany). Dicumy Peroxide (DCP) was provided by Shanghai Lingfeng Chem. Co. (China). Solvents as xylene, lsopropylalcohol, formic acid and acetone were analytic reagents. Polyamide 11 was supplied by Atochem. The density is 1.03×10^3 kg/m^3. The glass transition temperature (T_g) and melting point (T_m), measured by DSC, is about 38 °C and 184 °C, respectively. Poly (vinyl chloride) (PVC) was provided by Sinopec Qilu Co., Ltd. (China) in the form of powder with a molecular weight (M_w) of 6.25×10^4. Thermal additives added in PA11/PVC blends are dibasic and tribasic heat stabilizer, to improve the process temperature of PVC to180–190 °C.

Synthesis and purification of EVA-g-MAH

MAH and DCP were premixed proportionally in acetone and then mixed with EVA under vigorous stirring. After hours of acetone volatilization, the mixer was molten-reacted in HAAKE Rheocord at 175 °C with the rotor speed of 40 rpm and a reaction time of 10 min. EVA/MAH reactant was refluxed in xylene for 2 h to get rid of insoluble solids. The mixture in xylene was then dropped into acetone to deposit EVA-g-MAH and the unreacted EVA. The unreacted monomers and maleic anhydride homopolymer were dissolved in acetone. Deposit was washed several times with acetone. After this, the residues were dried under vacuum at 50 °C for 24 h.

FT-IR characterization of EVA-g-MAH

The purified residues and KBr were thoroughly mixed and pressed into thick films, then analyzed using an FTIR spectrometer (Nicolet 20DXB, Madison, WI) from 4000 cm^{-1} to 500 cm^{-1} with a 0.8 cm^{-1} resolution.

Titration

To compensate the FTIR characterization, the grafted MAH ratio of EVA-g-MAH was determined by titrimetry. 0.3 g EVA-g-MAH was dissolved in 50×10^3 mm^3 xylene during reflux. Then 5×10^3 mm^3 NaOH/ethanol solution $(0.05 \times 10^3$ mol/m$^3)$ was added, followed by further reflux for 10 more minutes.

HCl/Isopropylalcohol solution (0.05×10^3 mol/m³) was adopted for titration, using phenolphthalein as indicator. The following formula was used to calculate the grafting ratio:

$$\text{wt\%} = \frac{(N_1 V_1 - N_2 V_2 - A * W) * M}{1000 * 2 * W} * 100\%$$

where N_1 is the concentration of NaOH/ethanol solution; V_1 the volume of NaOH/ethanol solution; N_2 the concentration of HCl/Isopropylalcohol solution; V_2 the volume of HCl/Isopropylalcohol solution; M the maleic anhydride molecular weight, 98×10^{-3}; A the NaOH dissipation of EVA alcoholysis during titration, 4.6×10^3 mol/kg was determined in our experiment and W the sample weight.

The units of the quantities defined above are fundamental SI units.

Polymer blends preparation and mechanical testing

PA11, PVC, EVA-g-MAH and other additives were premixed proportionally in a mixing machine and were removed to mix in a internal mixer (XSS-300, Shanghai Light Industry Machinery Co., Ltd. China) at 185 °C and 40 rpm for 5 min and then were compressed to thick sheets through an external mixer(XK-160, Nanjing Rubber Mach. China). After that, 4-mm-thick sheets of these blends were made by a compression molding (QLB350 × 350 × 2, Wuxi No.1 Rubber & Plastic Works, China) for impact test.

Izod impact specimens were prepared according to ASTM D4812. Izod impact strength was obtained from unnotched specimens using an impact tester (Shanghai Wuzhong Instrument, JB6). Tensile properties were measured according to ASTM D638 using a tensile tester (RDT-30A, Shenzhen Reger Co. Ltd.) with computerized data acquisition. The testing was generally performed at a cross-head speed of 20 mm/min at room condition (20–25 °C and 30–40% RH, relative humidity).

DMA measurements

Dynamic mechanical analysis (DMA) data, storage modulus (E') and loss tangent (tan δ), were obtained under a multiwave dynamic tension mode at 10 Hz by Perkin-Elmer instruments DMA 7e. The specimen dimension was $20 \times 4 \times 1$ mm³ under a tensile model.

SEM morphology

The structure and morphology of the blends were studied using a scanning electron microscope (JSM-5610LV, JEOL, Datum Ltd., Tokyo, Japan). To clearly watch the phase structure, THF was used to etch PVC phase. Prior to SEM examination, the surfaces were coated with a layer of palladium.

Results and discussion

Characterization of EVA-g-MAH and its grafting ratio

FT-IR characterization of EVA-g-MAH

The reaction proportion of MAH/DCP was kept at 10/1 and MAH contents were 2–4% of EVA, based on literature conclusion [34]. Figure 1 is the spectrum of neat EVA (VA content 40%). Figure 2 is the spectrum of EVA-g-MAH at the proportion of 100/2/0.2 (EVA/MAH/DCP). Figure 3 is the spectrum of EVA-g-MAH at the proportion of 100/4/0.4 (EVA/MAH/DCP).

The characteristic peaks of MAH are 1856 cm⁻¹ and 1780 cm⁻¹, which attribute to symmetrical and asymmetrical stretching vibrations of the carbonyl groups (C=O) of cyclic anhydride [35–37]. It is not easy to identify the characteristic peaks of MAH, which is grafted onto EVA, because EVA and MAH possess the same C=O group [38]. Only peaks between 1700 cm⁻¹ and 1900 cm⁻¹ can better act as the evidence of MAH grafting onto polymer chains.

Comparing with peaks in Fig. 1, peaks at 1856 and 1781 cm⁻¹ in Fig. 2, peaks at 1857 and 1781 cm⁻¹ in Fig. 3 appear in neat EVA spectrum. Since the unreacted MAH gives rise to the absorption bands in the same region where the grafted anhydride does [39], it is of great importance to eliminate all unreacted MAH. Elimination of unreacted MAH can be verified by the disappearance of the characteristic absorption
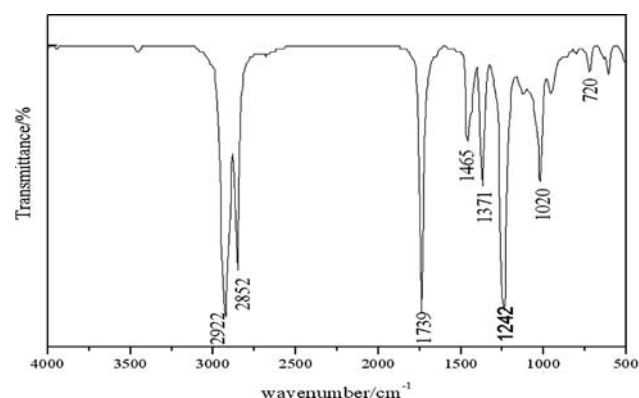

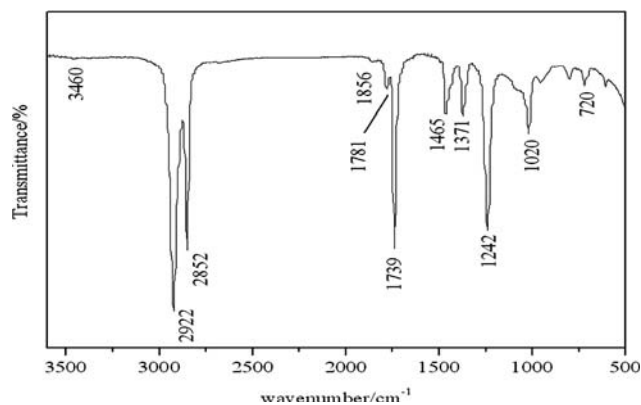Fig. 1 FTIR spectrum of neat EVA (VA content 40 %)

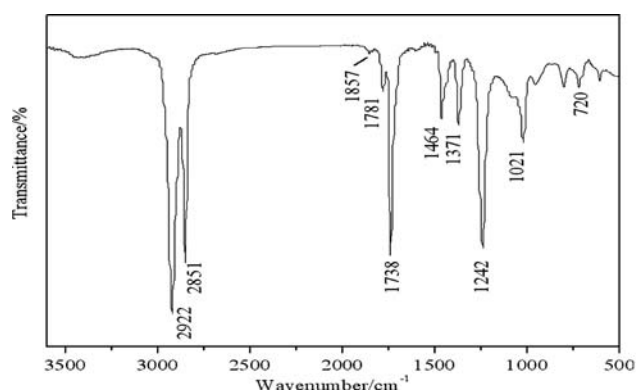Fig. 2 FTIR spectrum of EVA-g-MAH at the proportion of 100/2/0.2 (EVA/MAH/DCP)

Fig. 3 FTIR spectrum of EVA-g-MAH at the proportion of 100/4/0.4 (EVA/MAH/DCP)

band at 700 cm^{-1} assigned to the carbon/carbon double bond of MAH. In Figs. 2 and 3, no peaks appear at 700 cm^{-1}, confirming that the unreacted MAH has been extracted out during reflux. The new appeared peaks in Figs. 2 and 3 prove that MAH has been grafted onto EVA.

Grafting ratio of EVA-g-MAH from titration

The grafting ratio at different reaction proportion and temperature was determined by titration. Various grafting ratios are summarized in Table 1.

Reaction techniques affect greatly on the melting grafting reaction. Reaction temperature decides the half-life of initiator. Enhanced temperature will shorten the half-life of DCP, increasing its decomposing velocity and consequently an increased free radical concentration. This will promote the reaction and subsequently a higher grafting ratio. However, the high temperature will also promote crosslinking, which is unfavorable. The increase of temperature from 100 °C to 150 °C leads to higher grafting ratio, at all reaction

Table 1 Effect of reaction proportion and temperature on grafting ratio to EVA (VA 40%)

Proportion Temperature	100/2/0.2	100/3/0.3	100/4/0.4
100 °C	0.05%	0.12%	0.42%
150 °C	0.61%	1.24%	1.65%

proportion. The reflux by xylene did not leave any insoluble solids under these two reaction temperatures, indicating that there is no cross linking reaction.

Random incorporation of the vinyl acetate unit into polyethylene progressively hinders the ability of the polymer to crystallize. Higher VA content leads to much lower EVA crystallinity. This polar function group also promotes the grafting reaction, as can be seen from Table 2. EVA with 40 wt% VA content got higher grafting ratios at the same reaction temperature. When more DCP and MAH were added to EVA, the free radicals increased and the grafting ratios were enhanced.

However, the grafting ratio does not always increase with increasing MAH concentration. Higher concentration will increase the chance of auto polymerization. What's more, graft copolymer affects blends properties. As a compatibilizer, a moderate grafting ratio is enough. EVA whose VA content is lower that 30 wt% is immiscible with PVC, as mentioned in introduction. We select EVA with 40 wt% VA content and a grafting ratio of 1.65% to investigate the compatibilization effect of EVA-g-MAH.

Effect of EVA-g-MAH on the mechanical properties PA11/PVC blends

Figure 4 shows the stress–strain curves of the PA11/PVC (1:1) and PA11/PVC (3:1) blends during tensile testing. From the stress–strain curves we can see the variation of tensile strength, tensile modulus as well as elongation at break of materials. Particulars are plotted in the following figures.

The variations of the mechanical properties as a function of EVA-g-MAH content are illustrated in Fig. 5. It is indicated that at 15 wt% EVA-g-MAH concentration, PA11/PVC blends achieve maximum tensile strength, elongation at break, tensile modulus and impact strength. When EVA-g-MAH content is

Table 2 Effect of VA content on grafting ratio at settled temperature of 150 °C

Proportion VA content	100/2/0.2	100/3/0.3	100/4/0.4
18	0.42%	1.00%	1.70%
40	0.61%	1.24%	1.65%

Fig. 4 Tensile stress–strain curves of (**a**) PA11/PVC (1:1) blends; (**b**) PA11/PVC (3:1) blends. The curves represent various EVA-g-MAH contents at A: 0 wt%; B: 5 wt%; C: 10 wt%; D: 15 wt%; E: 20 wt%
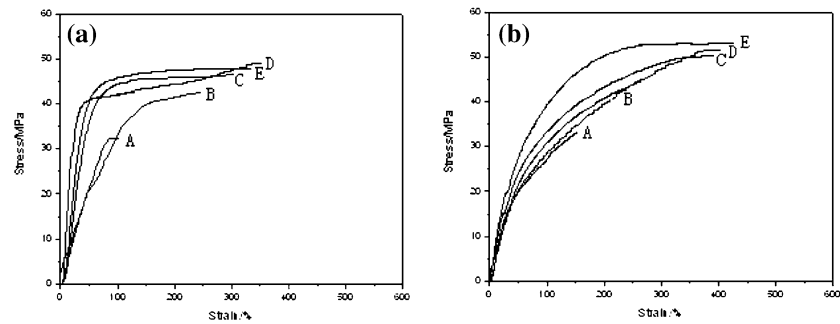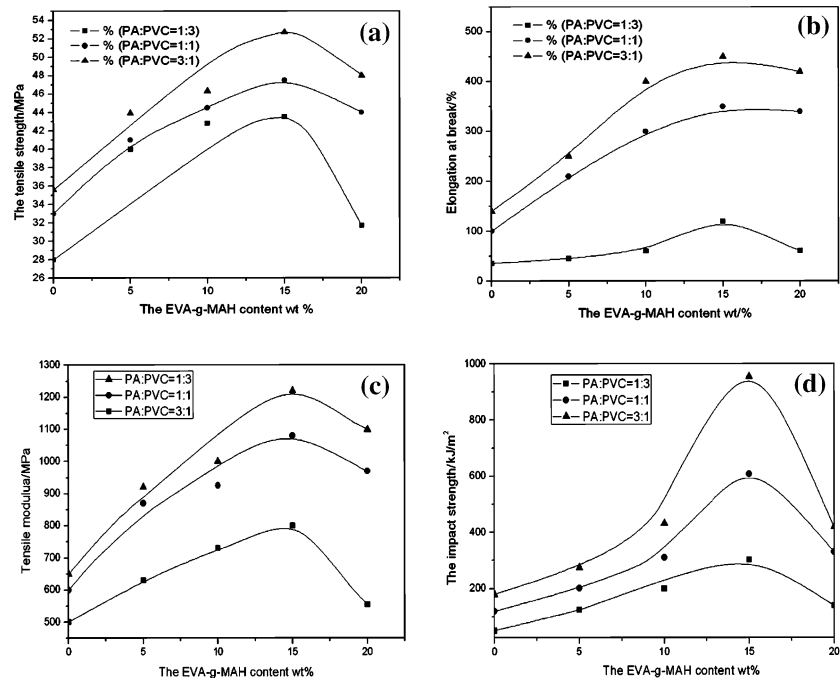
Fig. 5 Mechanical properties of PA11/PVC blends as a function of EVA-g-MAH content: (**a**) tensile strength; (**b**) elongation at break; (**c**) tensile modulus; (**d**) impact strength

higher than 15 wt%, the excess EVA-g-MAH is immiscible with PA11, consequently deteriorated compatibilization and mechanical properties. Anhydride functionality of EVA-g-MAH can react with the amine end of PA11 at the interface and in situ form copolymer at the interface. This copolymer reduces the interfacial tension, promotes better dispersion of PVC as well as adhesion between phases. When investigating the effect of PA11/PVC proportion on the compatibilization and mechanical properties of the blends, we kept EVA-g-MAH at a consistent content of 15 wt%.

Effect of PA11/PVC proportion on mechanical properties

Figure 6 is the stress–strain curves of the blends at different PA11/PVC ratio and consistent EVA-g-MAH content of 15 wt%. Figure 7 shows the various mechanical properties of PA11/PVC blends as a function of

PVC incorporation. Figure 7a shows that a small incorporation of PVC into PA11 gets a higher tensile strength than neat PA11. The tensile strengths of PA11/PVC blends decrease slightly with the increasing PVC contents. The tensile moduli increase sharply and the elongations at break decrease sharply. Before the incorporation of PVC as high as 50 wt%, some impact samples did not break even suffered great energy. The mechanical results indicate that the blends mechanical properties decrease slightly with the incorporation of PVC lower than 50 wt% content, and PVCs incorporation into PA11 can significantly decrease PA11 materials' cost with negligible performance losing.

Compatibilization mechanism of EVA-g-MAH in PA11/PVC blends

The grafting reactions in EVA copolymers may take place on the methyl group of the acetate moiety or on
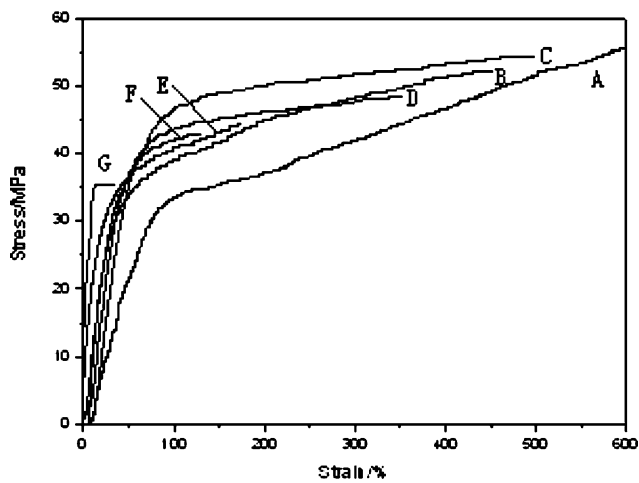
Fig. 6 Tensile stress–strain curves with different PA11/PVC proportion: A = 4/1 B = 3/1 C = 2/1 D = 1/1 E = 1/2 F = 1/3 G = 1/4

the tertiary C–H. Gaylord et al. [40] believed that these reactions occur preferentially on the methyl group. From the FTIR results and the titration analysis of the hydrolyzed product of EVA–MA, Soares et al. [34] concluded that the grafting reaction of MA into the EVA copolymer occurred predominantly on the tertiary C–H of the backbone, contrarily to the mechanism proposed by Gaylord et al. We take the conclusion by Soares to further discuss the compatibi-

lization mechanism of EVA-g-MAH in PA11/PVC blends.

Figure 8a schematically illustrates the graft reaction between PA11 and EVA-g-MAH. The in situ reaction formed copolymer promotes the compatibilization between PA11 and EVA-g-MAH. PVC and EVA-g-MAH are miscible. The polar carbonyls in VA functional group and maleic anhydride functional group can interact with the α-H of PVC. The α-hydrogen atoms in the maleic anhydride group can also interact with the electronegative chloride atoms in PVC macromolecule [31]. These intermolecular interactions further promote the PA11/PVC compatibilization. Figure 8b shows the schematic description for ideal interactions between PA11, PVC and EVA-g-MAH.

The compatibilizers aggregate at the phase interface, and in situ react with PA11 to form copolymer. These copolymers lower the interfacial tension, improving miscibility between components. The intermolecular interactions can lower system entropy, further improve the miscibility. The simple scheme of EVA-g-MAH compatibilization effect is summarized as:

$$A/C/B \longrightarrow \text{in-situ reaction} A/A\text{-}g\text{-}C/B$$

where A-g-C is the microphase separation compatibilizer; C and B have intermolecular interactions.

Fig. 7 Mechanical properties of PA11/PVC blends as a function of PVC content: (**a**) tensile strength; (**b**) elongation at break; (**c**) tensile modulus; (**d**) impact strength
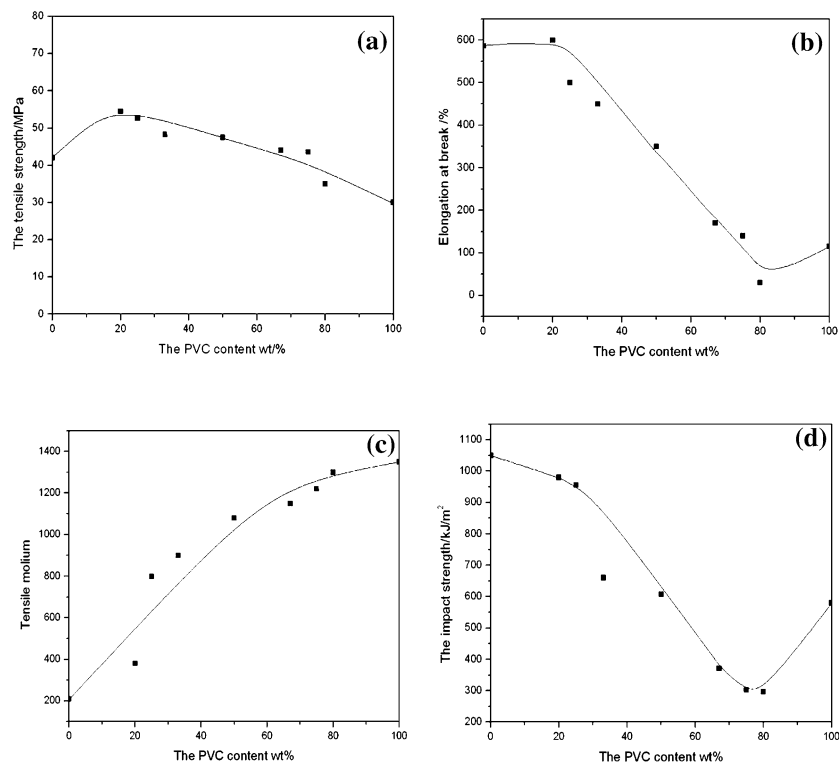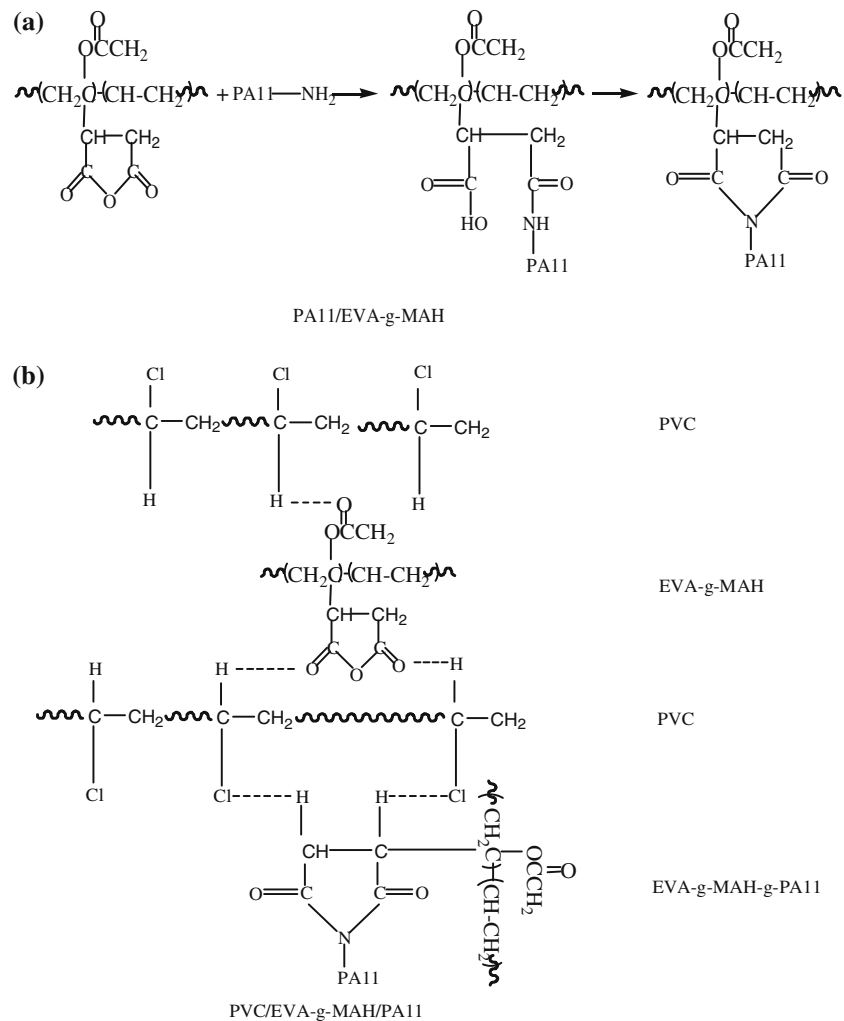
Fig. 8 Ideal schemes of: (**a**) reaction between PA11 and EVA-g-MAH; (**b**) intermolecular specific interactions between PA11 EVA-g-MAH and PVC

PA11/EVA-g-MAH

PVC

EVA-g-MAH

PVC

EVA-g-MAH-g-PA11

PVC/EVA-g-MAH/PA11

Dynamic mechanical properties of PA11/PVC blends

Figure 9 shows the compatibilization effect of EVA-g-MAH on dynamic mechanical properties of PA11/PVC blends. Tan δ curves in Fig. 9a illustrate the glass transition temperature (T_g) of PA11 and PVC compo-

nents in PA11/PVC (3:1) blends with and without the presence of EVA-g-MAH. The T_g of original PA11 and PVC used in this paper are 38 and 83 °C, respectively. In the absence of EVA-g-MAH, Tg of PA11 and PVC remain at 38 and 83 °C, respectively, indicating that components in the blends are immiscible. Whereas in the presence of EVA-g-MAH, T_g

Fig. 9 (**a**) Tan δ curves of PA11/PVC (3:1) blends: (A) without compatibilizer; (B) with 15 % EVA-g-MAH compatibilizer. (**b**) Storage moduli (E′) of (A) PA11; (B)PA11/PVC (3:1) with 15% EVA-g-MAH; (C) PA11/ PVC (3:1) without EVA-g-MAH; (D) PVC
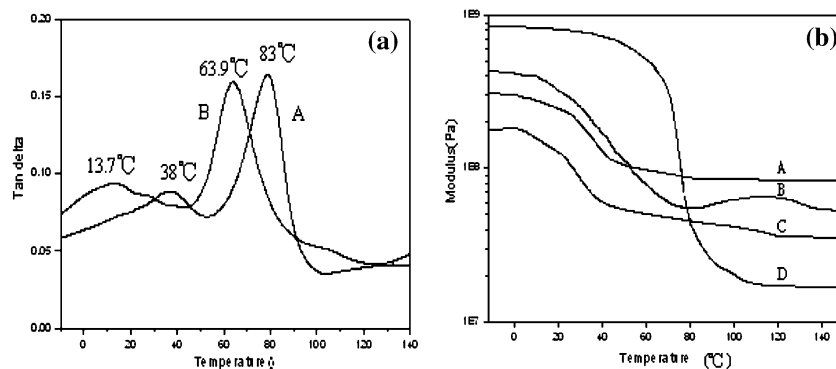
Fig. 10 (a) Tan δ curves of PA11/PVC blends: (A) PA11/PVC (1:3); (B) PA11/PVC (1:1); (C) PA11/PVC (3:1). (b) Storage moduli (E') of the PA11/PVC blends: (A) PA11; (B) PA11/PVC (3:1); (C) PA11/PVC (1:1); (D) PA11/PVC (1:3); (E) PVC
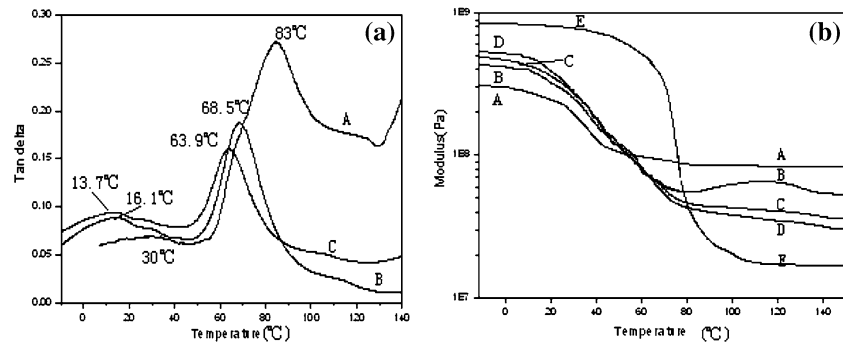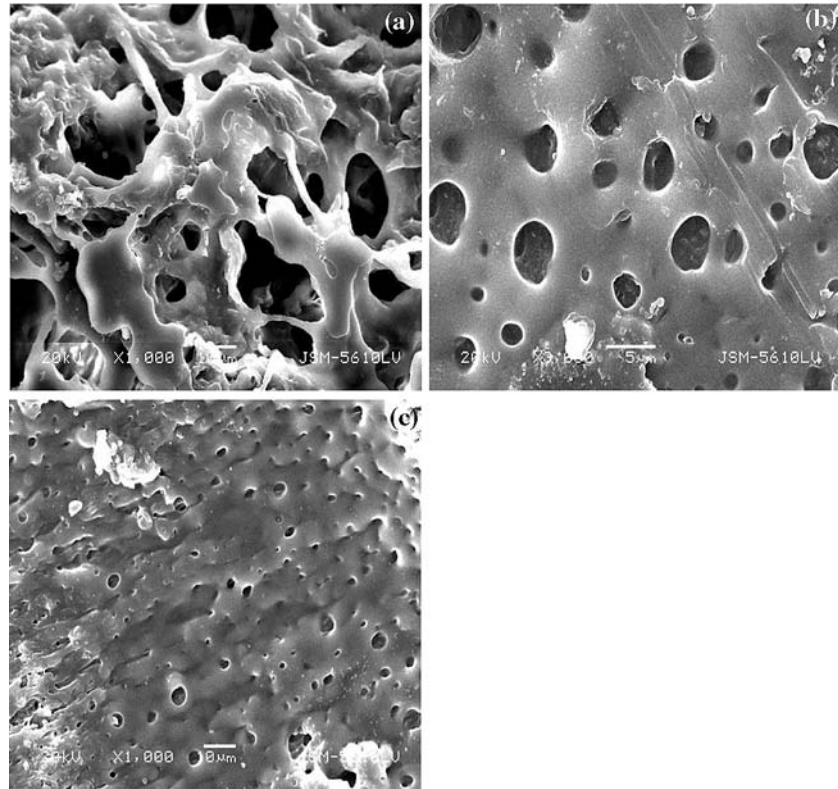

Fig. 11 SEM micrographs of uncompatibilized PA11/PVC blends: (a) PA11/PVC (1:3); (b) PA11/PVC (1:1); (c) PA11/PVC (3:1)


shifts to 13.7 and 63.9 °C for PA11 and PVC, respectively. The shifts imply improved compatibility of PA11/PVC by EVA-g-MAH.

Normally, the T_g of two individual components may shift reversely with the improved compatibilization, and the final single broad relaxation means the complete compatibilization. Whereas in our research, the improved compatibilization leads to the shift of both PA11 and PVC to a lower temperature T_g. The followings are the examination of this phenomenon. For a compatibilization PA11/PVC blends, the insert of PA11 chains into PVC chains would surely decrease the interaction of PVC chains, consequently a decreased T_g of PVC. For a polymer that has lower T_g than PVC and no intermolecular hydrogen bonds, the insert of PVC chains would likely to increase the T_g of

this polymer, providing that they are compatible. PA11 comprises 10 methylene groups, one carbonyl group, and one amide in the repeat unit. Unlike many other nylons, all carbonyl and amide groups in the PA11 chain interact to form hydrogen bonds, which contribute greatly to the molecular interaction [41]. The insert of PVC chains to PA11 chains destroys the intermolecular hydrogen bonds of PA11, thus the intermolecular interaction is not increased but decreased. The improved compatibilization of PA11/PVC thus leads to the lower temperature shift of T_g of PA11.

Figure 9b represents the storage modulus (E') as a function of increasing temperature. After compatibilization, moduli of PA11/PVC blends are moderate between pure PA11 and PVC, whereas, the modulus is much lower without compatibilizer. The influence of

Fig. 12 SEM micrographs of
15% EVA-g-MAH
compatibilized PA11/PVC
blends: (**a**) PA11/ PVC (1:3);
(**b**) PA11/ PVC (1:1); (**c**)
PA11/ PVC (3:1)
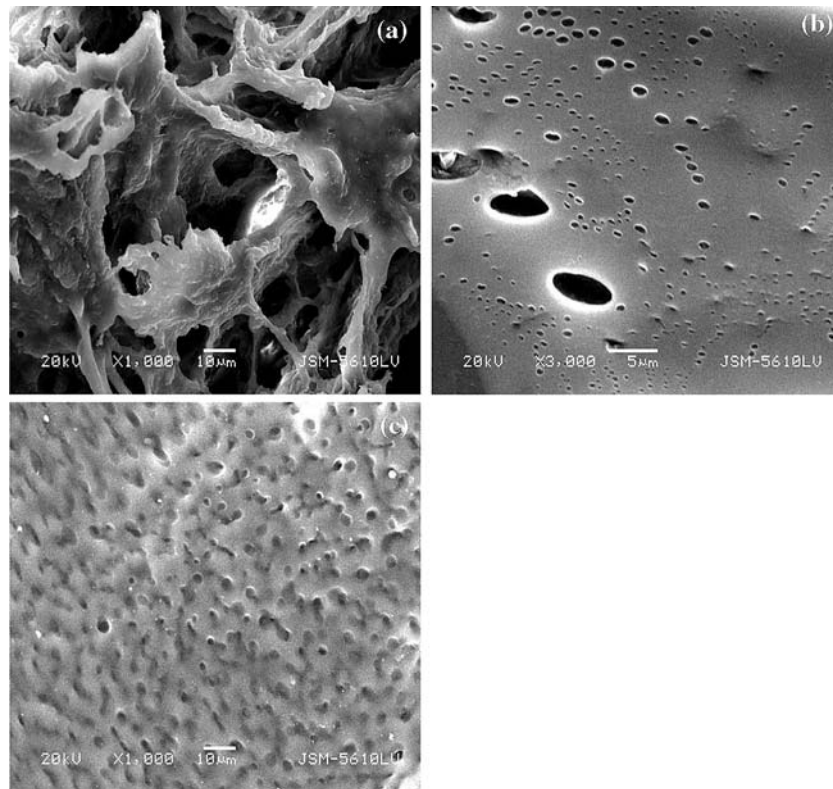
PA11/PVC ratio on the dynamic mechanical properties
of PA11/PVC blends is showed in Fig. 10. In Fig. 10a,
PA11/PVC (1:1) blends show T_g at 16.1 and 68.5 °C,
respectively. For PA11/PVC (3:1) blends, T_g locates at
13.7 and 63.9 °C. Increasing PA11 percentage in the
blends, the T_g of each component shifts to lower
temperature, implying much improved compatibility.
Figure 10b represents the storage modulus (E') as a
function of increasing temperature for the PA11/PVC
blends. EVA has a relatively low storage modulus. The
E' of the blends decreases dramatically at low temper-
ature, comparing with the storage modulus of neat
PVC. However, at higher temperature, the blends
maintain a relative high E' comparing with neat PVC.
The modulus was enhanced at high temperature.

Morphology of PA11/PVC blends

Figure 11 shows microstructures of PA11/PVC blends
without EVA-g-MAH compatibilizer. Figure 12 shows
microstructures of PA11/PVC blends compatibilized
by 15% EVA-g-MAH. The voids on the surfaces
represent the PVC phase, with has been etched by
THF. In our investigated proportion regions, PVC is
the dispersed phase and PA11 is the continuous phase,
even for PA11/PVC (1:3) blends. Without the presence
of EVA-g-MAH, PVC phase is less uniformly dis-
persed in PA11 phase and the surface is rougher. In

PA11/PVC (1:3) blends without compatibilizer, the
blends even show macro phase separation and exfoli-
ated to layers. The rough surface in Fig. 11a indicates
that PVC phase is not uniform and has a bad interface
with PA11 phase. The presence of EVA-g-MAH leads
to the reduction of PVC phase size and its uniform
distribution, as well as good interface interaction with
PA11 phase.

The microstructure also depends on PA11/PVC
ratio greatly, similar as the mechanical properties
dependence on components ratio. At PA11/PVC
(1:1) blends, PVC dispersed well, although big domain
regions of PVC still exit. PVC phase dispersed more
finely and uniformly in PA11/PVC blends with high
PA11 concentration, as can be seen from Fig. 12c.

Conclusion

EVA-g-MAH was specially synthesized and applied as
a compatibilizer to immiscible PA11/PVC blend sys-
tems. Mechanical properties indicate that the critical
EVA-g-MAH content is 15 wt% in the blends, to get
good performance. There are intermolecular interac-
tions between specific functional groups of EVA-g-
MAH and PVC, they are miscible. The in situ reaction
at PA11/PVC interfaces promotes the compatibiliza-
tion. Dynamic mechanical analysis and the fine disper-

sion of PVC from the SEM micrographs further prove the compatibilization. In PA11/PVC blends, PVC is a dispersed phase in the continuous PA11 phase in our investigated proportion regions. PA11/PVC combination affects PVC dispersion greatly. PVC incorporation into PA11 can significantly decrease PA11 materials cost with negligible performance losing.

References

1. Sung YT, Kum CK, Lee HS, Kim JS, Yoon HG, Kim WN (2005) Polymer 46:11844
2. Marcilla A, Gomez A, Reyes-Labarta JA (2001) Polymer 42:8103
3. Doak KW (1986) In: Mark HF, Bikales NM, Overberger CG, Menges G (eds) Encyclopedia of polymer science and engineering, vol 6. Wiley, New York, p 383
4. Soares BG, Alves FF, Oliveira MG, Moreira ACF, Garcia FG, Lopes MFS (2001) Eur Polym J 37:1577
5. Kim SJ, Shin BS, Hong JL, Cho WJ, Ha CS (2001) Polymer 42:4073
6. Cartasegna S (1986) Rubber Chem Technol 49:722
7. Steinkamp DG, Grail TJ (1975) U.S. Patent 3,862,265
8. Gaylord NG (1985) U.S. Patent 4,506,056
9. Gaylord NG, Mehta R (1988) J Polym Sci Part A: Polym Chem 26:1189
10. Ikkala OT, Holsti-Miettinen RM, Seppalla J (1993) J Appl Polym Sci 49:1165
11. Moon HS, Ryoo BK, Park JK (1994) J Polym Sci Polym Phys 32:1427
12. Arup RB, Anup KG, Shok MA (2001) Polymer 42:9143
13. Chris S, Chris M (1994) J Polym Sci Polym Phys 32:205
14. Deimedea VA, Fragoua KV, Koulouri EG, Kallitsis JK, Voyiatzis GA (2000) Polymer 41:9095
15. Dai KH, Kramer EJ, Frechetj MJ, Wilson PG, Moore RS, Long TE (1994) Macromolecules 27:5187
16. Auschra C, Stadler R, Voigt-Martin IG (1993) Polymer 34:2081
17. Auschra C, Stadler R, Voigt-Martin IG (1993) Polymer 34:2094
18. Gsell TC, Pearce EM, Kwei TK (1991) Polymer 32:1663
19. Liu SY, Zhang GZ, Jiang M (1999) Polymer 40:5449
20. Zhang GZ, Liu SY, Zhao HY, Jiang M (1999) Mater Sci Eng C 10:155
21. Liu SY, Zhu H, Jiang M, Wu C (2000) Langmuir 16:3712
22. Jiang M, Li M, Xiang ML, Zhou H (1999) Adv Polym Sci 146:121
23. Liu SY, Pan QM, Xiej W, Jiang M (2000) Polymer 41:6919
24. Lu X, Weiss RA (1991) Macromolecules 24:4381
25. Lu X, Weiss RA (1992) Macromolecules 25:6185
26. Charoensirisomboon P, Saito H, Inoue T, Weber M, Koch E (1998) Macromolecules 31:4963
27. Zakrzewski GA (1973) Polymer 14:347
28. Schurer JW, Boer A, Chall AG (1975) Polymer 16:201
29. Hickman JJ, Ikeda RM (1973) J Polym Sci: Polym Phys Ed 11:1173
30. Koleske JV, Lundberg RD (1969) J Polym Sci, Part A-2 7:795
31. Olabisi O, Robeson LM, Shaw MT (1979) Polymer–polymer miscibility. Academic Press, Inc
32. Robeson LMJ (1978) Polym Sci: Polym Lett 16:261
33. Lian YX, Zhang Y, Peng ZL, Zhang XF, Fan RL, Zhang YX (2001) J Appl Polym Sci 80:2823
34. Soares BG, Colombaretti RSC (1999) J Appl Polym Sci 72:1799
35. Wang SJ, Yu JG, Yu JL (2005) Polym Degrad Stab 87:395
36. Deng JP, Yang WT (2005) Eur Polym J 41:2685
37. Grigoryeva OP, Karger-Kocsis J (2000) Eur Polym J 36:1419
38. Kim SJ, Shina BS, Honga JL, Chob WJ, Ha CS (2001) Polymer 42:4073
39. De Roover B, Sclavons M, Carlier V, Devaux J, Legras R, Montaz A (1995) J Appl Polym Sci 33:829
40. Gaylord NG, Mehta M, Mehta R (1995) Antec. 1635
41. Zhang QX, Mo ZS (2001) Polym Bull 6:27